

Contrast Improvement of Chest Organs in Computed Tomography Images using Image Processing Technique

Yousif Mohamed Yousif Abdallah^{1*}, Magdolin Siddig²

¹College of Medical Radiological Science, Sudan University of Science and Technology

²Medical Radiology Department, National College For medical and Technical studies

Abstract

Image enhancement allows the observer to see details in images that may not be immediately observable in the original image. Image enhancement is the transformation or mapping of one image to another. The enhancement of certain features in images is accompanied by undesirable effects. We proposed that to achieve maximum image quality after denoising, a new, low order, local adaptive Gaussian Scale Mixture model and median Filter were presented, which accomplishes nonlinearities from scattering a new nonlinear approach for contrast enhancement of soft tissues in CT images using both clipped binning and nonlinear binning methods. The usual assumption of a distribution of Gaussian and Poisson statistics only lead to overestimation of the noise variance in regions of low intensity (small photon counts), but to underestimation in regions of high intensity and therefore to non-optimal results. The contrast enhancement results were obtained and evaluated using MatLab program in 50 CT images of the chest and abdomen from two CT studies. The optimal number of bins, in particular the number of gray-levels, is chosen automatically using entropy and average distance between the histogram of the original gray-level distribution and the contrast enhancement function's curve.

Key Words: Obstructive jaundice, management, mortality, morbidity.

INTRODUCTION

Image enhancement techniques are used to refine a given image, so that desired image features become easier to perceive for the human visual system or more likely to be detected by automated image analysis systems. Image enhancement allows the observer to see details in images that may not be immediately observable in the original image. This may be the case, for example, when the dynamic range of the data and that of the display are not commensurate, when the image has a high level of noise or when contrast is insufficient.^[1,2] Fundamentally, image enhancement is the transformation or mapping of one image to another. This transformation is not necessarily one-to-one, so that two different input images may transform in to the same or similar output images and medical images as illustrated in the figures after enhancement.^[3] More commonly, one may want to generate multiple enhanced versions of a given image this aspect also means that enhancement techniques may be irreversible. Often the enhancement of certain features in images is accompanied by undesirable effects. Valuable image information may be lost or the enhanced image may be a poor representation of the original. Further more enhancement algorithms cannot be expected to provide information that is not present in the original image. If the image does not contain the feature to be enhanced, noise or other unwanted image components may be inadvertently enhanced with out any benefit to the user. Pixel based enhancement techniques are transformations applied to each pixel with out utilizing specifically the information in the neighborhood of the pixel. Enhancement that can be achieved with multiple images of the same scene.^[4] A digital image is defined as a two-dimensional array of numbers that represents the real, continuous

spatial signal is sampled at regular intervals and the intensity is quantized to a finite number of the array is referred to as a picture element or pixel. The digital image is defined as a spatially distributed intensity signal $f(m, n)$, where f is the intensity of the pixel, and m and n define the position of the pixel, along a pair of orthogonal axes usually defined as horizontal and vertical. We shall assume that the image has M rows and N columns and that the digital image has P quantized levels of intensity (gray levels) with values ranging from 0 to $P-1$. The histogram of an image, commonly used in image enhancement and image characterization, is defined as a vector that contains the count of the number of pixels in the image at each gray level. A useful image enhancement operation is convolution using local operators, also known as Kernels. Considering a Kernel $w(k, l)$ to be an array of $(2k+1+2+1)$ coefficients where the point $(k, l) = (0,0)$ is the center of the Kernel, convolution of the image with the Kernel is defined by:

$$G(m, n) = w(k, l) * f(m, n) \text{ =Type equation here.}$$

Where $g(m, n)$ is the out come of the convolution or out put image. To convolute an image with a kernel, the kernel is centered on an image pixel (m, n) , the point-by-point products of the kernel coefficients and corresponding image pixels are obtained, and the subsequent summation of these products is used as the pixel value of the out put image $g(m, n)$ is obtained by operating the same operation on an pixels of original image. A convolution kernel can be applied to an image in order to effect of specific enhancement operation or change in the image characteristics. This typically results in desirable attributes being amplified and undesirable attributes being suppressed. The specific values of the kernel coefficients depend on the different types of enhancement that may be desired. Attention is needed at the boundaries of the image where parts of the kernel extend beyond the input image. One approach is to simply use the portion of the kernel that overlaps the input image. This approach can, however, lead to artifacts in the boundaries of the out put image.^[5]

The forward or inverse Fourier transform of an $N \times N$ image, computed directly with the preceding definitions, requires a

Address for correspondence*

Yousif Mohamed Yousif Abdallah

College of Medical Radiological Science, Sudan University of Science and Technology

Email: yousifmohamed@sustech.edu

number of complex multiplications and additions proportional to N^2 . By decomposing the expressions and eliminating redundancies, the fast Fourier transform (FFT) algorithm reduces the number of operations to the order of N

$$\text{Log}_2 N^{[5]}$$

The computational advantage of the FFT is significant and increases with increasing N . when $N = 64$ the number of operation are reduced by an order of magnitude and when $N = 1024$, by two orders of magnitudes.^[6]

Pixel Operation

Although intensity scaling can be very effective in enhancing image information present in specific intensity bands, often information is not available a priori to identify the use full intensity bands. In such cases, it may be more use full to maximize the information conveyed from the image to the user by distributing the intensity information in the image as uniformly as possible over the available intensity band.^[7-9] This approach is based on the approximate realization of information – theoretic approach in which the normalized histogram of the image is interpreted as the probability density function of the intensity of the image. In histogram equalization, the histogram of the input image is mapped to a new maximally-flat histogram. The histogram is defined as $h(i)$, with 0 to $p-1$ gray levels in the image. The total number of pixels in the image, $M*N$, is also the sum of all the values in $h(i)$. Thus, in order to distribute most uniformly the intensity profile of the image, each bin of the histogram should have a pixel count of $(M*N)/p$. It is, in general, possible to move the pixel with a given intensity to another one, resulting in an increase in the pixel count in the new intensity bin. On the other hand, there is no acceptable way to reduce or divide the pixel count at a specific intensity in order to reduce the pixel count to the desired $(M*N)/P$. In order to achieve approximate uniformity, the average value of the pixel count over a number of pixel values can be made close to the uniform level.^[10-11] A simple and readily available procedure for distribution of the pixels in the image is based in the normalized cumulative histogram, defined as

$$H(j) = 1/M \cdot \sum_{i=0}^j h(i) \quad j=0,1,\dots, p-1$$

The normalized cumulative histogram can be used as a mapping between the original gray levels in the image and the new gray levels required for enhancement. The enhanced image $g(m, n)$ will have a maximally uniform histogram if it is defined as

$$g(m, n) = (p-1) \cdot H(f(m, n))$$

A. Noise Suppression by Mean Filtering

Mean filtering can be achieved by convolving the image with $(2K+1) \times (2L+1)$ Kernel where each coefficient has a value equal to the reciprocal of the number of coefficients in the Kernel. For example, $L=K=1$, we obtain

$$w(k, l) = \frac{1}{9} \begin{bmatrix} 1 & 1 & 1 \\ 1 & 1 & 1 \\ 1 & 1 & 1 \end{bmatrix}$$

Referred to as the 3×3 averaging kernel or mask. Typically, this type of smoothing reduces noise in the image, but at the expense of the sharpness of edges (4), (5), (12), (13). Note

that the size of the kernel is a critical factor in the successful application of this type of enhancement. Image details that are small relative to the size of the kernel are significantly suppressed, while image details are significantly larger than the kernel size are affected moderately. The degree of noise suppression is related to the size of the kernel, with greater suppression achieved by larger kernels.^[11,7,12,13]

Median filtering is a common nonlinear method for noise suppression that has unique characteristics. It does not use convolution to process the image with a kernel of coefficients. Rather, in each position of the kernel frame, a pixel of the input image contained in the frame is selected to be out put pixel located at the coordinates of the kernel center. The kernel frame is centered on each pixel (m, n) of the original image, and the median value of pixels with in the kernel frame is computed. The pixel at the coordinates (m, n) of the out put image is set to this median value. In general, median filters don't have the same smoothing characteristics as the mean filter. Features that are smaller than half the size of the median filter kernel are completely removed by the filter. Large discontinuities such as edges and large changes in image intensity are not affected in terms of gray level intensity by the median filter, although their positions may be shifted by a few pixels. This nonlinear operation of the median filter allows significant reduction of specific types of noise. For example, "shot noise" may be removed completely from an image without attenuation of significant edges or image characteristics.^[14]

MATERIALS AND METHODS

For Computed tomography machines (CT) each film was scanned using digitizer scanner then treat by using image processing program (MatLab), where the enhancement and contrast of the image were determined. The scanned image was saved in a TIFF file format to preserve the quality of the image. The data analyzed used to enhance the contrast within the soft tissues, the gray levels which can be redistributed both linearly and nonlinearly using the gray level frequencies of the original CT scan. The data was analyzed by using statistical package, Statistical Package for Social Studies (SPSS) under windows.

The Fourier transform is a representation of an image as a sum of complex exponentials of varying magnitudes, frequencies, and phases. The Fourier transform plays a critical role in a broad range of image processing applications, including enhancement, analysis, restoration, and compression.

If $f(m, n)$ is a function of two discrete spatial variables m and n , then the two-dimensional Fourier transform of $f(m, n)$ is defined by the relationship.

$$F(\omega_1, \omega_2) = \sum_{m=-\infty}^{\infty} \sum_{n=-\infty}^{\infty} f(m, n) e^{-j\omega_1 m} e^{-j\omega_2 n}$$

Figure

The variables ω_1 and ω_2 are frequency variables; their units are radians per sample. $F(\omega_1, \omega_2)$ is often called the frequency-domain representation of $f(m, n)$ $F(\omega_1, \omega_2)$. is a complex-valued function that is periodic both in ω_1 and ω_2 , with period 2π . Because of the periodicity, usually only the range $-\pi \leq \omega_1, \omega_2 \leq \pi$ is displayed. Note that $F(0,0)$ is the sum of all the values of $f(m, n)$. For this reason, $F(0,0)$ is often called the constant component or DC component of the Fourier transform. (DC stands for direct current; it is an electrical engineering term

that refers to a constant-voltage power source, as opposed to a power source whose voltage varies sinusoidally.) The inverse of a transform is an operation that when performed on a transformed image produces the original image. The inverse two-dimensional Fourier transform is given by

$$f(m, n) = \frac{1}{4\pi^2} \int_{\omega_1=-\pi}^{\pi} \int_{\omega_2=-\pi}^{\pi} F(\omega_1, \omega_2) e^{j\omega_1 m} e^{j\omega_2 n} d\omega_1 d\omega_2$$

Figure

Roughly speaking, this equation means that $f(m, n)$ can be represented as a sum of an infinite number of complex exponentials (sinusoids) with different frequencies. The magnitude and phase of the contribution at the frequencies (ω_1, ω_2) are given by $F(\omega_1, \omega_2)$. The Fourier transform provides the spectral representations of an image, which can be modified to enhance desired properties.

Visualizing the Fourier Transform

To illustrate, consider a function $f(m, n)$ that equals 1 within a rectangular region and 0 everywhere else. To simplify the diagram, $f(m, n)$ is shown as a continuous function, even though the variables m and n are discrete (Fig.1).

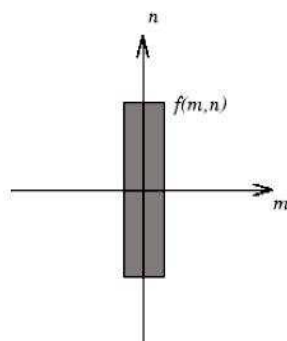


Figure 1. Visualizing the Fourier Transform (MatLab R2009m)

The Fig.2 shows, as a mesh plot, the magnitude of the Fourier transform, $F(\omega_1, \omega_2)$, of the rectangular function shown in the preceding figure. The mesh plot of the magnitude is a common way to visualize the Fourier transform.

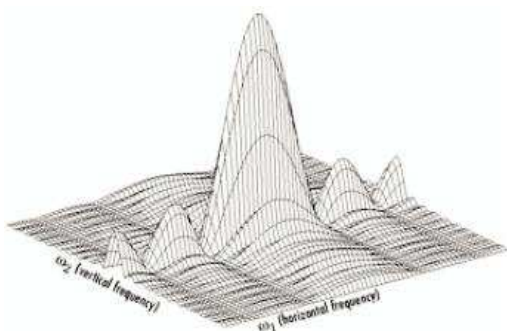


Figure 2. A mesh plot, the magnitude of the Fourier transform, $F(\omega_1, \omega_2)$, (MatLab R2009m)

Magnitude Image of a Rectangular Function

The peak at the center of the plot is $F(0,0)$, which is the sum of all the values in $f(m, n)$. The plot also shows that $F(\omega_1, \omega_2)$ has more energy at high horizontal frequencies than at high vertical

frequencies. This reflects the fact that horizontal cross sections of $f(m, n)$, are narrow pulses, while vertical cross sections are broad pulses. Narrow pulses have more high-frequency content than broad pulses.

Another common way to visualize the Fourier transform is to display $\log |F(\omega_1, \omega_2)|$ as an image, as shown in Figure 2.

Log of the Fourier Transform of a Rectangular Function

Using the logarithm helps to bring out details of the Fourier transform in regions where $F(\omega_1, \omega_2)$ is very close to 0.

RESULTS

This is an experimental study deals with propose a new approach for image enhancement technique using noise reduction technique (noise variance) and different median Filters in CT images and reduction of the redundancy in the image data using image processing technique (MatLab version R2009a). In addition to highlight the role of the proposed approach (noise variance) by preservation of the image's overall look, preservation of the diagnostic content in the image and detection of small and low contrast details in the diagnostic content of the image and to highlight the role of using image processing technique in Radiology. Gaussian mixture models are formed by combining multivariate normal density components. For information on individual multivariate normal densities. In Statistics Toolbox software, mixture models of the gmdistribution class are fit to data using expectation maximization (EM) algorithm, which assigns posterior probabilities to each component density with respect to each observation. Gaussian mixture models are often used for data clustering. Clusters are assigned by selecting the component that maximizes the posterior probability. Like k-means clustering, Gaussian mixture modeling uses an iterative algorithm that converges to a local optimum. Gaussian mixture modeling may be more appropriate than k-means clustering when clusters have different sizes and correlation within them. Creation of Gaussian mixture models are described in the Gaussian Mixture Models section of Probability Distributions. Thus, in real CT images one can find a significant coherence of the noise with the image content. To illustrate the problem two CT images acquisitions are dedicated; one image (Fig.3) form Chest area scan technique and other image form sand another one is unenhanced image for the same area (Fig.4). The figure 5 shows an idealistic view of CT images in figure 4, which needs to be enhanced and free from the mixture of noise.

DISCUSSION

The most important criterion of Radiology images is enhancement and resolution to differentiate between to or more closely tissues. There are many problems due to absence of enhancement of soft tissues in CT images and reduction of the redundancy in the image data. Redundant data is usually caused by large ranges of gray levels being used to represent images, which actually require significantly fewer gray levels. Image enhancement allows the observer to see details in images that may not be immediately observable in the original image. Image enhancement is the transformation or mapping of one image to another. The enhancement of certain features in images is accompanied by undesirable effects Valuable image information may be lost or the enhanced image may be a poor representation of

the original. Computed tomography is a medical imaging technique, which employees tomography, where digital geometry processing is used to generate a three dimensional image of an object from a large series of two dimensional image taken around a single axis of rotation. In computed tomography, the image is made by viewing the patient via x- ray imaging from numerous angle, by mathematically reconstructing the detailed structures and displaying the reconstructed image on a video monitor. Contemporary with the development of viable CT scanner, rotate/rotate, systems and to avoid the sensitivity to ring artifacts, a design was developed using a stationary detector ring and a rotating X-ray tube. Because the reduced motion seemed consistent with a reduction in complexity, this geometry is known as the fourth generation. The stationary detector requires a larger acceptance angle for radiation, and is therefore more sensitive to scattered radiation than the 3rd generation geometry. Fourth generation geometries also require a larger number of detector cells and electronic channels (at a potentially higher cost) to achieve the same spatial resolution and dose efficiency as a 3rd generation system. Medical images are often deteriorated by noise due to various sources of interference and other phenomena that affect the measurement processes in imaging and data acquisition systems. The nature of the physiological systems under investigation and the procedures used in imaging also diminish the contrast and visibility of details. For example, planer projection nuclear medicine images obtained using a gamma camera as well as single photon- emission computed tomography (SPECT) as severally degraded by Poisson noise that's inherent in the photon emission and counting processes. Intensity scaling can be very effective in enhancing image information present in specific intensity bands, often information is not available a priori to identify the use full intensity bands. In such cases, it may be more use full to maximize the information conveyed from the image to the user by distributing the intensity information in the image as uniformly as possible over the available intensity band. This approach is based on the approximate realization of information – theoretic approach in which the normalized histogram of the image is interpreted as the probability density function of the intensity of the image. In histogram equalization, the histogram of the input image is mapped to a new maximally-flat histogram. The histogram is defined as $h(i)$, with 0 to $p-1$ gray levels in the image. The total number of pixels in the image, $M*N$, is also the sum of all the values in $h(i)$. Thus, in order to distribute most uniformly the intensity profile of the image, each bin of the histogram should have a pixel count of $(M*N)/p$. It is, in general, possible to move the pixel with a given intensity to another one, resulting in an increase in the pixel count in the new intensity bin. On the other hand, there is no acceptable way to reduce or divide the pixel count at a specific intensity in order to reduce the pixel count to the desired $(M*N) /P$. In order to achieve approximate uniformity, the average value of the pixel count over a number of pixel values can be made close to the uniform level. This is an experimental study deals with propose a new approach for image enhancement technique using noise reduction technique (noise variance) and different median Filters in CT images and reduction of the redundancy in the image data using image processing technique (MatLab version R2009a). In addition to highlight the role of the proposed approach (noise variance) by preservation of the image's overall look, preservation of the diagnostic content in the image and detection of small and low contrast details in the diagnostic content of the image and to highlight the role of using image processing technique in Radiology. In real CT images one can find a significant coherence of the noise with the image content. To illustrate the problem two CT images acquisitions are

dedicated; one image (Fig.4) form Chest area scan technique and other image form sand another one is unenhanced image for the same area (Fig.3). The Fig.5 shows an idealistic view of CT images in Fig.6, which needs to be enhanced and free from the mixture of noise.

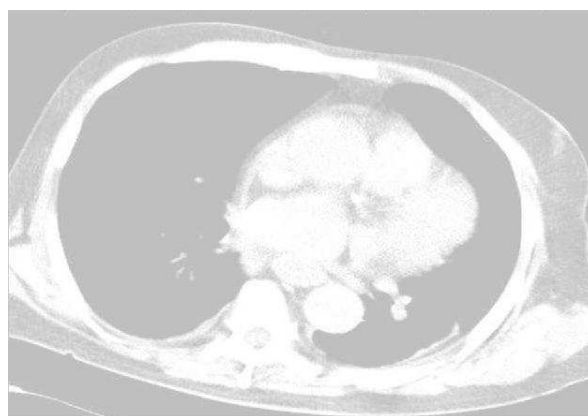


Fig.3. Shows CT image (original image)



Fig.4. Shows enhanced CT image using median Filter (median, 10)

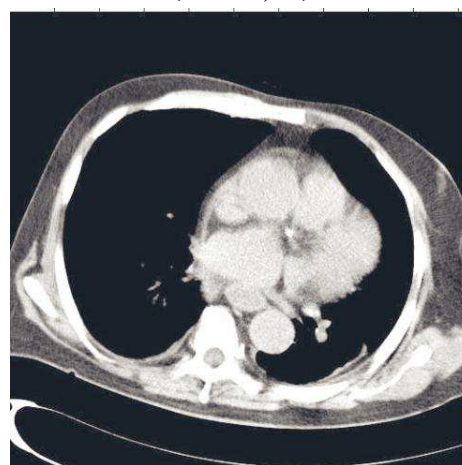


Fig.5. Shows enhanced CT image using median Filter (median, 15)

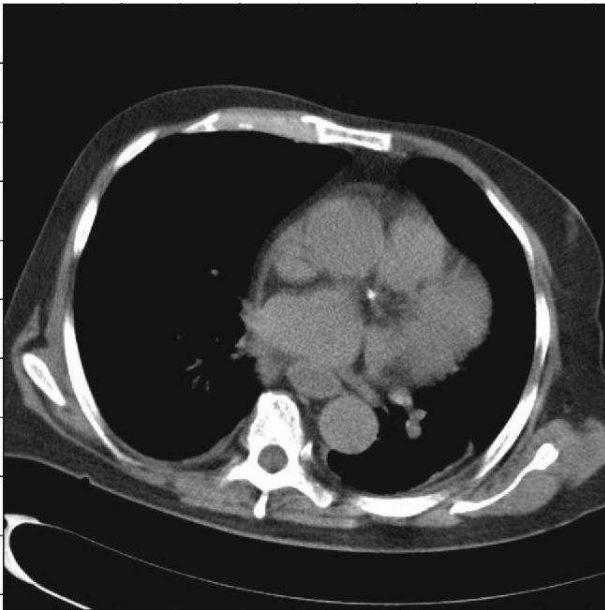


Fig.6. Shows enhanced CT image using median Filter (median, 20)

REFERENCES

1. Adelson, E.H., Bergen, J.R. 1991. "The plenoptic function and the elements of early vision", In *Computation Models of Visual Processing*, M. Landy and J.A. Movshon, eds., MIT Press, Cambridge, 1991, pp. 3-20.
2. Arvo, J., 1994, *The Irradiance Jacobian for Partially Occluded Polyhedral Sources*, Proc. ACM SIGGRAPH, ACM Press, pp. 335-342.
3. Yousif M.Y. Abdallah, 2010, *Computed verification of Light and radiation Field Size on Coblac-60*, Lambert Publisher Press, Germany, P.p. 34-66
4. Ball, J., Moore, A., 1997, *Essential physics for radiographers*, 3rd edition, Blackwell Scientific, Oxford.
5. Ball, J., Price, T., 1995, *Chesney's radiographic imaging*, 6th edition, Blackwell Scientific, Oxford.
6. Buehler, C., Bosse, M., McMillan, L., Gortler, S., Cohen, M., 2001, *Unstructured Lumigraph rendering*, Proc. ACM SIGGRAPH, ACM Press.
7. Farr, R., Allisy-Roberts, P., 1997, *Physics for medical imaging*, W.B. Saunders, London.
8. Fritsch D.S.; Chaney E.L.; McAuliffe M.J.; Raghavan S.; Boxwala A.; Earnhart J.R.D., 1995, *International Journal of Radiation Oncology, Biology, Physics*, Volume 32, Number 971, , pp. 217-217.
9. Georgiev, T., Zheng, C., Nayar, S., Curless, B., Salesin, D., Intwala, C., 2006, *Spatio-angular Resolution Trade-offs in Integral Photography*, Proc. EGSR 2006.
10. Levoy, M., Ng, R., Adams, A., Footer, M., Horowitz, M., 2006, *Light field microscopy*", ACM Transactions on Graphics (Proc. SIGGRAPH), Vol. 25, No. 3.
11. Matusik, W., Pfister, H., 2004, *3D TV: a scalable system for real-time acquisition, transmission, and autostereoscopic display of dynamic scenes*, Proc. ACM SIGGRAPH, ACM

Press.

12. Yang, J.C., Everett, M., Buehler, C., McMillan, L., 2002, *A real-time distributed light field camera*, Proc. Eurographics Rendering Workshop 2002.
13. Abdelnour, A.F., Nehmeh, S.A., Pan, T., Humm, J.L., Vernon, P., Schoder, H., Rosenzweig, K.E., Mageras, G.S., Yorke, E., Larson, S.M., Erdi, Y.E.: *Phase and amplitude binning for 4D-CT imaging*, Journal of Medical Physics and Biology, vol.52, P.p.3515-3529
14. Ahn, S., Yi, Y. Suh, J. Kim, S. Lee, S. Shin, S. Shin, and E. Choi. (2004). "A feasibility study on the prediction of tumour location in the lung from skin motion", *British Journal of Radiology*, Vol.77(919):P.p.588-596.
15. Alheit H, Dornfeld S, Winkler C, Blank H and Geyer P, 2000, *Stereotactic guided irradiation in prostatic cancer using the ExacTrac-System (BrainLab)*, Journal of Radiotherapy and Oncology, Vol.56 (Suppl. 1):P.p.107
16. Allen AM, Siracuse KM, Hayman J A and Balter JM, 2004, *Evaluation of the influence of breathing on the movement and modeling of lung tumors*, International Journal of Radiation Oncology and Biology Physics, Vol.58:P.p.1251-7
17. Arnold, V.I, 1997, *Mathematical Methods of Classical Mechanics*, 2nd edn, Springer, England.
18. Artignan X, Smitsmans M H P, de Bois J, Lebesque J V, van Herk M and Bartelink, 2002, *On-line ultrasound image guidance for radiotherapy of prostate cancer: the impact of image acquisition on prostate displacement*, Journal of Radiotherapy and Oncology, Vol.64 (Suppl. 1):P.p.279
19. Artignan X, Smitsmans M H P, Lebesque J V, Jaffray D A, van Herk M and Bartelink, 2004, *Online ultrasound image guidance for radiotherapy of prostate cancer: impact of image acquisition on prostate displacement*, International Journal of Radiation Oncology and Biology Physics, Vol.59:P.p.595-601
20. Aubrey J-F, Beaulieu L, Girouard L-M, Aubin S, Tremblay D, Laverdiere J and Vigneault, 2004, *Measurements of intrafraction motion and interfraction and intrafraction rotation of prostate by three-dimensional analysis of daily portal imaging with radiopaque markers*, International Journal of Radiation Oncology and Biology Physics, Vol.60,P.p.30-9
21. Aznar M C, Sixel K E and Ung Y C, 2000 *Feasibility of deep inspiration breath hold combined with intensity modulated radiation treatment delivery for left sided breast cancer* Proc., 42th Annual ASTRO Meeting, International Journal of Radiation Oncology and Biology Physics, Vol.48 (Suppl.)P.p.297
22. Balter J M, Litzenberg D W, Brock K K, Sanda M, Sullivan M, Sandler H M and Dawson L A, 2000, *Ventilatory movement of the prostate during radiotherapy*. Proc., 42th Annual ASTRO Meeting, International Journal of Radiation

Oncology and Biology Physics, Vol.48 (Suppl.)P.p.167

23. Balter J M, Wright J N, Newell L J, Friemel B, Dimmer S, Cheng Y, Wong J, Vertatschitsch E and Mate T P, 2005, Accuracy of a wireless localization system for radiotherapy, *International Journal of Radiation Oncology and Biology Physics*, Vol.61, P.p.933–937
24. Balter J, Wright N, Dimmer S, Friemel B, Newell J, Cheng Y and Mate T, 2003, Demonstration of accurate localisation and continuous tracking of implantable wires, *International Journal of Radiation Oncology and Biology Physics*, Vol.57, P.p.264
25. Balter, J. M., K. L. Lam, C. J. McGinn, T. S. Lawrence, and R. K. Ten Haken, 1998, Improvement of CT-based treatment-planning models of abdominal targets using static exhale imaging, *International Journal of Radiation Oncology and Biology Physics*, vol.41(4):P.p.939–943.
26. Barnes E A, Murray B R, Robinson D M, Underwood L J, Hanson J and Roa W H Y, 2001, Dosimetric evaluation of lung tumour immobilization using breath hold at deep inspiration, *International Journal of Radiation Oncology and Biology Physics*, Vol.50, P.p.1091–1098
27. Barnes, E. A., B. R. Murray, D. M. Robinson, L. J. Underwood, J. Hanson, and W. H. Roa, 2001, Dosimetric evaluation of lung tumor immobilization using breath hold at deep inspiration, *International Journal of Radiation Oncology and Biology Physics*, vol.50(4):P.p.1091–1098.
28. Beckham, W. A., P. J. Keall, and J. V. Siebers, 2002, A fluence-convolution method to calculate radiation therapy dose distributions that incorporate random set-up error, *Journal of Medical Physics and Biology*, vol.47 (19):P.p.3465–3473.
29. Beg, M.F., Miller, M.I., Troune, A., Younes, L.: Computing large deformation metric mappings via geodesic flows of diffeomorphisms. *International Journal of Computer and Visualization*, Vol.61-P.p.139-157
30. Berbeco R I, Mostafavi H, Sharp G C and Jiang S B 2005a Towards fluoroscopic respiratory gating for lung tumours without radiopaque markers, *Journal of Medical Physics and Biology*, vol.50, P.p.4481–4490